On the Impact of Time-varying Acoustic Channels on Routing Protocols for Underwater Networks

Beatrice Tomasi*, Giovanni Toso*‡, Paolo Casari*‡, Michele Zorzi*‡

*Department of Information Engineering, University of Padova — via Gradenigo 6/B, 35131 Padova, Italy
‡Consorzio Ferrara Ricerche — via Saragat 1, 44122 Ferrara, Italy
E-mail: {firstname.lastname}@dei.unipd.it

Abstract—We evaluate and compare the performance of source routing and flooding as a function of the network density, when employed in a static underwater acoustic network with time-varying channel conditions. First, we present field observations, highlighting different patterns of channel variability. Then, by feeding time series of environmental conditions into a ray tracer, we derive time-varying realistic channel realizations as would be perceived by a non-coherent receiver. Moreover, we propose a simple analytical approach, which relates the distance between two relay nodes, the time-variability of the link, and the reactiveness of the considered source routing algorithm.

We show that a critical hop distance can be identified, depending on the timing of the source routing protocol and on the statistics of the channel dynamics, after which source routing reacts too slowly with respect to the rate of variability of the channel quality. These results are corroborated by simulation runs, from which we derive the performance of source routing and flooding in different shallow water scenarios, highlighting which algorithm should be preferred.

Index Terms—Underwater acoustic networks, time-varying channels, source routing, flooding, performance comparison.

I. INTRODUCTION

Underwater acoustic communications enable several applications of both civilian and military interest, such as environmental monitoring and coastal surveillance. These applications often rely on network communications over multihop topologies. Recently, the community working on underwater acoustic communications has developed techniques and algorithms (e.g., see [1]) that mitigate the frequency and time-selectivity of underwater acoustic channels. Other studies investigated the dynamics of the channel quality in the presence of diverse environmental conditions. These works often involve observation intervals that are relevant for both point-to-point and network communications. Studies such as [2]–[7] aim at investigating which environmental parameters cause a set of channel-related metrics to vary over time. The presented results convey information about, e.g., the periods of time over which significant channel variations are to be expected, and are useful for the design both of network deployments and of communication protocols.

In the same vein, in this paper we present a study on how correlated time-varying channel conditions affect the performance of routing protocols in shallow-water acoustic networks. In particular, we will investigate the interplay among the acoustic propagation delay, the coherence time of the link quality and the time required by the protocols to exchange control messages (e.g., the route discovery and route reply signaling). More specifically, we focus on two different paradigms, namely source routing and flooding, which are based on different mechanisms and require a different amount of coordination and overhead. Furthermore, we consider different network scenarios, where we vary the network deployment area and relate the response time of the routing protocol to the correlation time of the link quality. This makes it possible to formulate several considerations. For instance, we can describe the maximum multihop communication distance, guaranteeing that the path remains stable in the interval of time between two subsequent route establishments. In turn, this leads to design guidelines for routing protocols whereby, e.g., the search for fresh routes is forced whenever such maximum distance is reached along a multihop path.

To the best of our knowledge, similar contributions are missing in the literature. Many simulation studies exist, e.g., [8], [9]. These works present simulation studies of different networking protocols in three-dimensional network scenarios, and employ an acoustic ray tracer in order to compute channel power gain realizations. However, they do not account for frequency selectivity and time-variability, that are widely recognized as critical for the performance of network communications. This also holds for [10], where both simulation and experimental results are shown for a specific scenario, but environmental data are not presented, thus making it impossible to generalize the results to similar environmental conditions.

Our approach differs from [8]–[10], since we i) observe the channel quality fluctuations, measured during different experiments; ii) investigate the relationship between the coherence time of the links, the distance between two relay nodes, and the response time of the routing protocols (consisting of both the overhead transmission time and the propagation delay); iii) confirm the insight provided by such analysis using network simulations.

We remark that the obtained results will be useful for both network deployment design and protocol design. In particular, given the changes of the channel quality over time at a specific deployment, by using our approach one can evaluate which routing protocol is more suitable for the given scenario. In addition, from a channel modeling perspective, our work

provides a first study highlighting what channel characteristics should be represented in a channel model suitable for studies related to protocol and deployment design.

A. State of the art

In this section, we provide an overview of the state of the art on the channel variability observed over different time intervals in several scenarios.

The results concerning the acoustic and environmental data collection during June-July 2003 in Kauai (HI) are summarized in the following. In [2], it was observed that receivers placed at a shallower depth experienced higher Bit Error Rate (BER) when the transmitter was deployed close to the sea bottom. In [3], the authors confirm, on average, the results in [2], and further investigate two cases: when the water is mixed (no thermocline) and when the water is stratified (and thus presents an apparent thermocline). In the former case, the performance of communications at the bottom is comparable with that measured near the surface, whereas in the latter case, since the acoustic energy is trapped inside the deep layers of the water column, the communications performance improves with increasing depth. In [4], the authors show that even though shallower water layers are characterized by a lower SNR, they show limited dynamics (mainly due to surface conditions), whereas bottom receivers are affected by wider SNR dynamics (mainly due to the fluctuations of the sound speed profile).

In [5], the authors study a very shallow water scenario (maximum depth 15 m). The data set was collected off the Delaware Bay in September. Both the source and the receivers were located close to the bottom. First, it was observed that in this very shallow water scenario, the time-varying channel conditions were mainly induced by surface waves. Moreover, the authors showed that an almost periodic behavior of the arrivals in the impulse response could be measured in the presence of a calm sea surface. A similar result can be found in [11], where the authors consider the SPACE08 data set, collected off the coast of Martha's Vineyard in a very shallow water scenario during October 2008.

In [7] the authors consider the KAM08 experiment, carried out off the coast of Kauai in 2008. The authors measured the communications performance when the transmitter is deployed at different depths, in particular above or below the thermocline. They show that the configuration exhibiting the worst communications performance is obtained by placing the source close to the surface.

All these works highlight the importance of the analysis and characterization of the time-varying channel conditions in stationary links. The results, shown in the referenced works, represent first evaluations of the link quality dynamics over intervals of time pertaining to communication systems and networking protocols. For this reason, we aim at evaluating the performance of two routing protocols in underwater acoustic time-varying links.

II. TIME-VARYING UWA CHANNEL

In this section, we present the time series of the channel quality at stationary links, both measured during different experiments and obtained via a ray tracer. The observed and computed time-varying channel conditions indicate that communication performance may vary over intervals of time pertaining to networking protocols, e.g., a few minutes, thus motivating the following study on the impact of these fluctuations on two types of routing algorithms.

A. Time-varying channel quality observed during experiments

Recently, several research groups have conducted experiments, consisting in transmitting and recording acoustic signals under water. Such experiments are characterized by different durations, timing and locations. These data sets serve for evaluating the performance of different communication systems in real coastal scenarios. As also outlined in Sec. I-A, the analysis of this data has highlighted that the quality of a static link exhibits fluctuations, whose dynamics are environment-dependent. However, identifying and quantifying the environmental conditions causing such time-varying behavior are subjects of ongoing research.

We present here the time series of the SNR estimates. Specifically we focus on three experiments, namely, SPACE08, SubNet09, and KAM11, which have been described in [11]–[13], respectively. These experiments lasted several days, thus making it possible to evaluate long-term channel quality fluctuations at stationary links.

It is worth noticing that the SNR is estimated differently according to the employed communication system. In fact, during both SPACE08 and KAM11, the transmitted signals were sent according to a coherent modulation scheme: for these data sets, we compute the average SNR at the output of an equalizer, whose parameters are indicated in [14] and [15], for SPACE08 and KAM11, respectively. On the other hand, several chirp pulses were employed during SubNet09: we make use of these chirps to estimate the instantaneous values of the SNR, as it would be measured by a non-coherent receiver.

Fig. 1 shows the time series of the output SNR over three minutes during SPACE08 and KAM11. The specific characteristics of the two deployment areas make the dynamics of the SNR very different. As shown in Fig. 1, during SPACE08, the output SNR has more limited dynamics than that observed during KAM11 over the three minute interval of time. An explanation of this lies in the different propagation conditions. In fact, in SPACE08 transmitters and receivers were deployed in a very shallow water area (water depth 15 m), whereas during KAM11 the water column was 100 m-deep. This may translate into different environmental factors affecting the propagation, thus leading to different dynamics. In particular, in [11] the authors highlighted the relationship between the observed dynamics and the time-varying surface conditions. It has been observed that at certain surface (and wind) conditions, the channel quality follows the time variability induced by the interaction between acoustic waves and
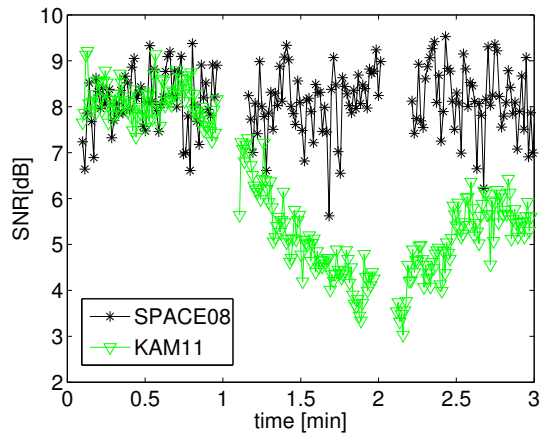
Fig. 1. Time series of output SNR during KAM11 at 3000 m on Julian date 188, represented with a black line, and during SPACE08 at receiving system 3 (200 m) on Julian date 292, shown with a green line.

Fig. 2. Time series of instantaneous SNR during SubNet09, on May 31, 2009, at receiver 2 (40 m below the surface) and transmitter 1 (1500 m).

the surface. However, the presence of a line of sight path makes the SNR quite stable over intervals of a few minutes, whereas the fluctuations of surface-reflected arrivals give rise to small drops around the average, as shown in Fig. 1. On the other hand, during KAM11, the time and space-varying sound speed profile significantly affected the propagation, thus also causing different channel quality dynamics. In fact, the fluctuation of the average value is larger than that observed in SPACE08, whereas the short-term oscillations around this average are smaller. A similar evaluation was performed on the data collected during SubNet09, for which, however, the instantaneous SNR values were measured only once every 30 seconds. For this reason, in Fig. 2, we show a time series over two hours. It can be noticed that the channel quality exhibits large fluctuations throughout the observed time interval. Similarly to KAM11 (we recall that the water depth was 80 m), the sound speed profile may play an important role in the acoustic propagation and its time-varying behavior for static links. However, due to the slow sampling rate of the channel quality, we are unable to evince the exact dynamics over intervals of time, e.g., a few minutes, pertaining to networking protocols.

Therefore, in light of these observations, we aim at evaluating how such fluctuations impact the performance of networking protocols for different topologies and link lengths. In fact, the combination of long propagation delays and a small available bandwidth (which implies long packet durations) makes underwater acoustic communications and networks prone to such channel fluctuations as those shown in Figs. 1 and 2. In particular, we want to verify whether or not longer links suffer more from channel fluctuations.

From a modeling point of view, reproducing these fluctuations for different scenarios and nodes placements is not a trivial task. However, we cannot use experimental traces for networking simulations, since they are specific to a single location, and this is in contrast with the possibility of measuring the protocol performance for varying link lengths.
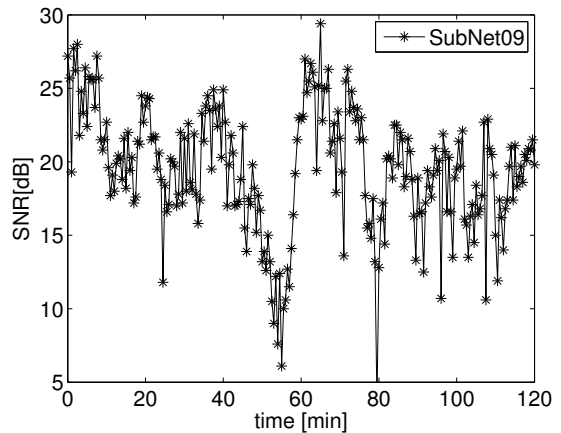
Moreover, since the channel gain is also a function of space, average performance has to be computed over different node deployments. For this reason, we resort to a simplified, though sufficiently accurate approach, which consists in computing the channel gain through a ray tracer. The details of this approach are presented in the next section.

B. Time-varying channel quality computed through ray-tracing

The channel variability perceived by a non-coherent receiver can be well approximated using Bellhop [16]. To do this, we employ the set of sound speed profiles (SSPs) measured during KAM11, and use it as an input to Bellhop. In order to model the other relevant environmental parameters, we consider a flat surface and bottom, and geoacoustic parameters typical of a rocky-muddy sea bottom. We focus on an interval of 8 hours in the KAM11 dataset, which includes one SSP sample every 5 s. For each sample, we compute the complex amplitude-delay profile of the acoustic channel as a function of the depth of the transmitter and of the receiver, as well as their range.[1] The amplitude-delay profile is post-processed, for each transmitter depth d_{tx}, receiver depth d_{rx} and transmitter-receiver range R, by summing the complex amplitudes of all arrivals, and by taking the square magnitude of the resulting sum to yield the channel power gain. With this information and by knowing the transmitted power, the transmit frequency and the system bandwidth, the SNR can be derived. Since the SSP changes over time (see Fig. 3), the channel power gain also changes. Fig. 4 exemplifies the fluctuation of the SNR over three underwater links, where the transmitter and the receiver are set at the same depth ($d_{tx} = d_{rx} = 5$, 50, or 95 m) and $R = 1500$ m. A window of 2 hours (out of the 8 hours depicted in Fig. 3) is considered. The three SNR curves show a very similar behavior, whereby the average SNR is stable

---

[1]Similar to the Bellhop jargon and akin to [17, Ch. 3], the range is defined as the planar distance between the nodes, i.e., as the distance projected on a plane parallel to the sea floor.
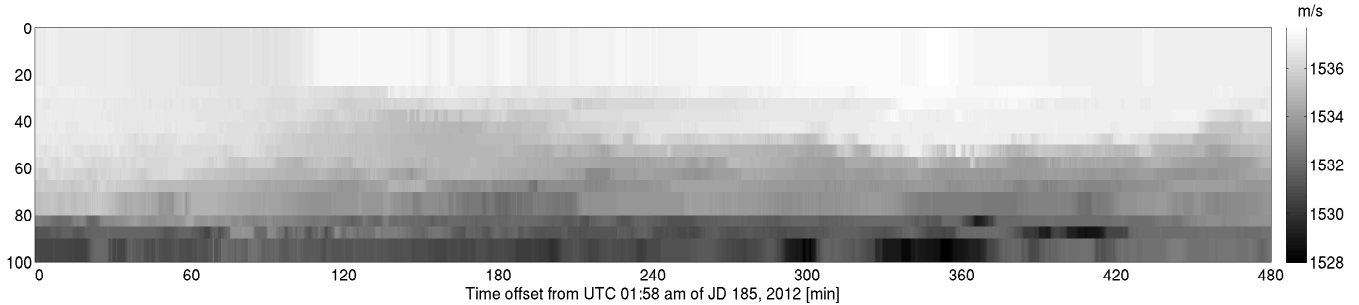
Fig. 3. Time series of the SSP measured once every 5 s for 8 hours during JD 185 of 2012. Darker shades of grey correspond to a lower sound speed. These values of the SSP are typical of a downward-refractive environment.
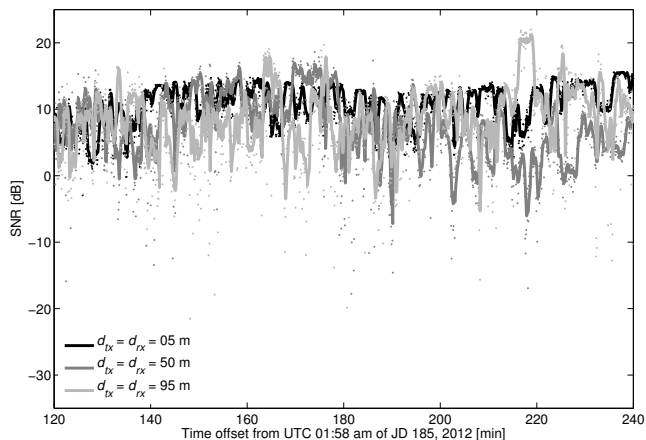
Fig. 4. SNR in dB as a function of time, $R = 1500$ m. The transmitter and the receiver are placed at the same depth; the traces show very similar behaviors. For each data set, the values of the SNR are shown as dots of the respective grey shade; a moving average taken over 6 samples (30 s) highlights the trend of the curves.
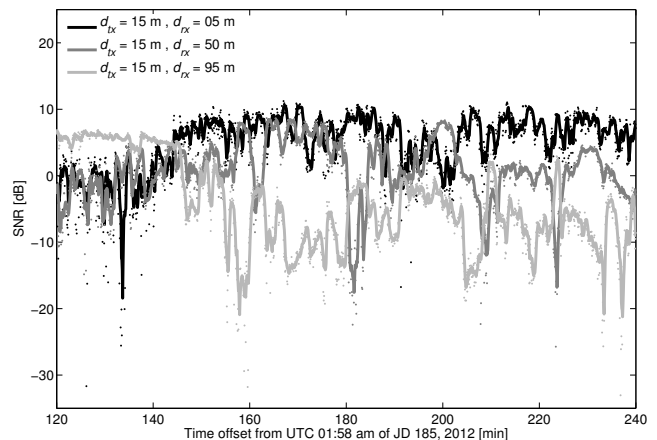
Fig. 5. SNR in dB as a function of time, $R = 3000$ m, $d_{\mathrm{tx}} = 15$ m, whereas d_{rx} is 5, 50 or 95 m. For each data set, the instantaneous values of the SNR are shown as dots along with their 6-sample moving averages, like in Fig. 4. All traces show periods of stability with minor local oscillations, as well as occasionally deeper fades.

in the long term, but local oscillations of 10 to 20 dB (peak-to-peak) are observed over intervals of around 3 min. Some deep fading events where the SNR decreases below 0 dB are also experienced by the links at 50 m and 95 m of depth. Fig. 5 shows a slightly different setup, where the transmitter is placed at $d_{\mathrm{tx}} = 15$ m and the receiver is at a range of $R = 3000$ m, at a depth $d_{\mathrm{rx}} = 5$, 50, or 95 m. The long-term difference between the values of the SNR over the three links is more remarkable in this case, although local variations of similar size, as in Fig. 4, also occur. Unlike in Fig. 4, however, we note that the dispersion of the SNR realizations around the moving average is smaller. In turn, this suggests that the oscillations of the SNR are mainly due to the confinement of the acoustic energy in different water layers, rather than to instantaneous changes in the interference pattern of the arrivals at the receiver. For example, the deep fade experienced for $d_{\mathrm{rx}} = 95$ m at around 155 min is mainly due to the fact that the sound speed between 40 and 60 m of depth is lower than around 120 min: this makes the propagation locally more uniform, decreasing the downward refraction of the acoustic wave and thereby reducing the amount of energy that reaches

the receiver. On the contrary, the instants of lower sound speed in the surface layers have a minor impact in this respect.

III. ANALYSIS, SIMULATION, AND RESULTS

In this section, we evaluate the performance of two types of routing algorithms: source routing and flooding. In particular, we aim at quantifying the impact of time-varying channel conditions and different network deployment areas on these routing algorithms. Moreover, by comparing their performance, we also provide recommendations on which algorithm works better in a given scenario.

We proceed as follows. First, we describe the protocols in Section III-A. Then, we propose a simple model in Section III-B, suitable for providing insight on the relationship among the reach of the links, the time-varying channel conditions, and the reactiveness of the source routing protocol. In Section III-C, we provide a detailed description of the simulation scenario, and we discuss the obtained results in terms of throughput, end-to-end delivery delay, and energy consumption.

A. Routing protocols

In this paper we consider two different routing protocols: a baseline flooding approach, whereby each node simply retransmits every data packet it receives with no coordination, and a reactive, distributed approach based on source routing, called Source routing for Underwater Networks (SUN).

SUN works as follows. The protocol separately addresses the behavior of two entities: sinks and nodes. Sinks are passive entities since their only tasks are (i) to periodically send probe messages in broadcast, in order to communicate their presence to the nodes within their communications range and (ii) to receive data packets. All other nodes can send data, ask for paths, answer path requests, act as relays and notify broken routes. In particular, the nodes receiving sink probes are called "end nodes" and answer path requests on behalf of the sink. The sink sends probes periodically, hence the set of end nodes is periodically refreshed: this also provides support for sink mobility.

In SUN, every node maintains a buffer with packets waiting to be forwarded. This includes both packets generated by the node and packets forwarded on behalf of other neighbors. An agent checks the buffer periodically, and if any packets are present, they are served according to a First-In-First-Out (FIFO) policy. The behavior of the agent is different according to the hop count of the node: end nodes (hop count 1) send the packets directly to the sink without further inquiry; the nodes with hop count equal to 0 do not know any valid path to the sink, and therefore start a path discovery process (described later); the nodes with hop count greater than 1 are not neighbors of the sink, but are aware of a valid path to the sink, which can hence be reached via multihop relaying. In this case, the full route to be followed is specified within the packet header.

The path discovery process works similarly to wireless radio source routing: a node starts the process by sending a path request, which is flooded until any end nodes are reached. Every node that retransmits a path request writes its own address in the header of the packet, hence forming a complete route as the request makes progress towards the sink. (Care is taken so that no node re-forwards the same path request twice, thereby avoiding loops.) At this point, each end node creates a path reply packet, which is sent back through the reverse of the route written in the header of the path request.

A node may receive multiple replies to the same path request. In this case, the node chooses the best route according to a given metric. In this work, the route with the lowest hop count is chosen (ties are broken by picking the route reply that was received first). The nodes can store valid routes and use them to replace any broken routes. However, all routes have an expiry time (set here to 12 minutes): if a path request is received and all known routes have expired, a fresh path request is issued.

For efficiency reasons, SUN is given full control over link layer retransmissions. Among other advantages, this allows SUN to perform error control only over data packets, and not over all control packets (something that would happen if error control were completely delegated to the data link layer). In case a data packet is correctly delivered to its next hop, an ACK is sent to the transmitter, and the forwarding process continues. In case of errors, the transmitter will see that the ACK is missing via the expiry of an ACK timeout, and will retransmit the data packet. In this paper we allow 1 retransmission. If this fails as well, the node will infer that the path is broken, and will notify the issue to the nodes upstream in the route by sending a path error packet. This makes it possible to perform a fresh route discovery and come up with a valid route.

B. Analytical model

The model proposed in this section is suitable for representing the relationship among the link length, the channel time-variability and the reactiveness of the routing protocol. In this section, we only consider the source routing algorithm, SUN, since the performance of the flooding algorithm is independent of the channel fluctuations. In fact, the flooding algorithm consists of making every node a relay. Broadly speaking, the algorithm neglects the possibility of a "best" route selection, and therefore the problem of the validity over time of that route does not arise. On the contrary, before transmitting the data packet, a source routing algorithm establishes the best path according to a given metric, which also depends on the link quality. In this case, the validity of the established path may vary, even in a static network, due to the time-varying link quality, as observed in Sec. II.

We consider a linear topology, along which nodes are deployed equally separated by a distance R. In the following, we assume that the Medium Access Control (MAC) protocol is a Carrier Sense Multiple Access (CSMA) scheme. For the sake of the analysis, this translates into a negligible delay introduced by the MAC layer. This would not be the case if, for example, a request to send/clear to send scheme were used. Another assumption is that the durations of control packets, which include both acknowledgments and path requests, are negligible with respect to the duration of the data packets and the propagation delays. The total number of nodes is indicated as N and it consists of a source, a destination and $N-2$ relay nodes. We define the *reactiveness* of the protocol, ρ, as the inverse of the maximum end-to-end delivery delay, T, which in the worst case corresponds to the longest path between source and destination, i.e., in the considered linear network when each node in the line is a relay. This end-to-end delivery delay, which includes both the path discovery and the data packet delivery, can be expressed as:

$$T = \frac{(N-2)RTT}{M} + (N-1)(t_{\text{data}} + RTT), \quad (1)$$

where M is the number of packets that can be delivered between two path establishments, RTT is the one-hop round trip time and t_{data} is the duration of the data packet. The round trip time depends on the hop distance, R, between two neighboring nodes, as $RTT = 2R/c$, where c is the
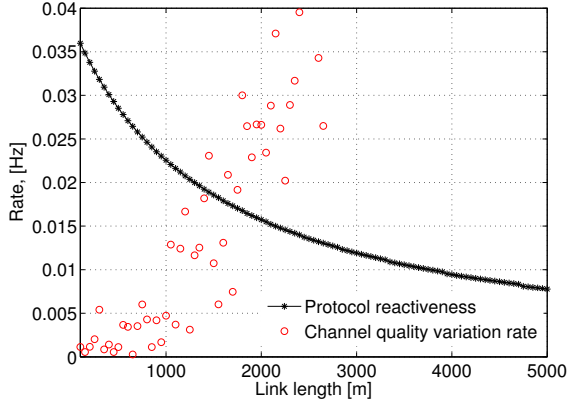
Fig. 6. Relationship between the protocol reactiveness as a function of nodes distance compared with the variability rate of the communications performance in red circles, here indicated as channel quality rate.

Fig. 7. Schematic representation of the simulation scenario as seen from above. Only the source on the left generates packets, which are routed to the sink on the right through the relays in between. The area in the middle is subdivided into 12 cells of volume $L \times L \times 95$ m^3. All nodes are deployed at the same depth of 45 m.

sound speed. Therefore, we express the reactiveness of SUN as a function of the link length, R, and the length of a data packet, t_{data}, which is constant. In order to have a stable reliable path, ρ should not be less than the variability rate of the communication performance. This means that the selected route remains the best candidate, according to a given metric, for the whole time interval between two consecutive path establishments.

Fig. 6 shows ρ as a function of the distance, when the network has a linear topology, $N = 14$ nodes and $t_{\text{data}} = 2$ s. Moreover, the routing protocol establishes the paths every 12 minutes. This parameter determines the variable M in (1). The red circles represent the channel quality variation rate measured from the channel gain time series computed by the ray tracer. In order to compute the variability rate of the channel quality, we measure the average time spent above a channel gain region (between -65 and -60, where the latter corresponds to an SNR of 5 dB) between two consecutive crossing times. As shown in Fig. 6, the channel quality variation rate becomes greater than the reactiveness of the protocol, when the link length is between 1600 and 1700 m. This distance can be considered as a critical link length for a source routing protocol, when the channel (and environmental) conditions vary as those shown in the example represented in Fig. 6. Therefore, by using the proposed approach, it is possible to extract general recommendations on which routing protocol should be employed in specific scenarios, defined by both the time-varying conditions and the network density, or equivalently the length of the links.

From the shown results, we can say that a reactive routing is not affected by time-varying channel conditions as long as the link length is less than about 1700 m. Beyond such distance, the protocol performance may suffer due to the time-varying channel conditions. In the following section, we evaluate and compare the performance of both SUN and a flooding routing protocol through simulations, in order to validate the insight provided in this section.
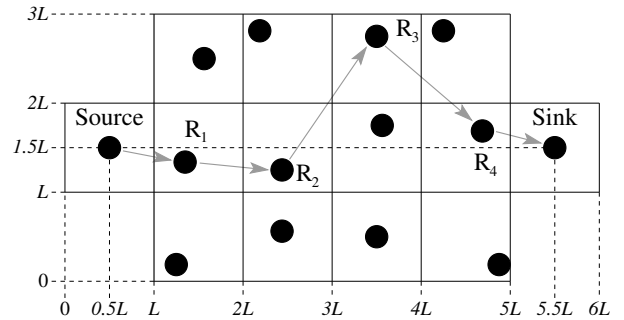
C. Simulation scenario and results

We implemented both the SUN protocol and the flooding routing algorithms in the NS-Miracle simulator [18]. In order to employ the channel power gain traces, derived in the study of Section II-B, we wrote a new physical layer module that imports these time series into NS-Miracle. Moreover, we assume a uniform underwater acoustic field, so as to make the computed time series of the power gains a sufficient description of the channel dynamics. This means that the power gain over any link depends only on the source and receiver depths, and on their range. Even though this assumption is not necessarily verified in practice, it still works as an approximation, and allows us to draw some significant conclusions on the behavior of the routing protocols. In order to model the performance of the link layer, we assume that the packets are transmitted using a modulation scheme with a spectral efficiency of 0.5, whereby a bandwidth of 8 kHz is allowed to achieve a bit rate of 4000 bps. The transmit power is set to 180 dB re μPa. By employing the channel gain realizations discussed in Section II-B and by computing the noise power using the empirical equations in [19], [20], an estimate of the Signal-to-Noise Ratio (SNR) is obtained. This SNR estimate is employed to compute the packet error probability via the Binary Phase Shift Keying (BPSK) error equations, assuming independent bit errors. The power of any interfering signal is treated as noise.

Our deployment follows the scheme in Fig. 7, where the network area is observed from above. There are a total of 14 nodes, of which two are the source and the sink (on the left and right, respectively). The network is 95 m-deep, and is divided into cells of volume $L \times L \times 95$ m^3, where L is the length of the side of each cell. The source and the sink are centered in the leftmost and rightmost cells, respectively; the other nodes are randomly deployed in the remaining 12 cells, one node per cell. All nodes are deployed at a depth of 45 m. This results in link behaviors such as those exemplified in Fig. 4, and makes it possible to evaluate the routing performance in the spirit of Section III-B, by ensuring a similar behavior for the links over time, while still retaining the short term variability that mostly
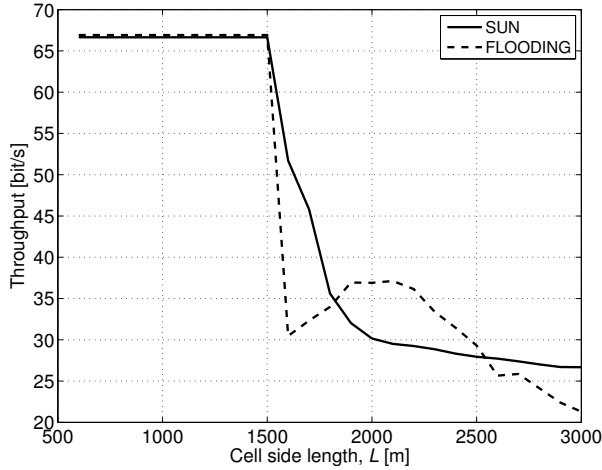
Fig. 8. Throughput as a function of the cell side length L for the SUN and the flooding protocols. The local increase of the flooding throughput around $L = 2000$ m is due to a favorable balance between transmission errors, leading to the injection of fewer packet replicas in the network, and the reduced interference that results.

Fig. 9. End-to-end delivery delay as a function of the cell side length L for the SUN and the flooding protocols. For $L \geq 1500$ m, the link variability unfavorably affects the stability of the routes, forcing SUN to perform route discovery more often. This results in longer delays for the packets that correctly reach the sink.

influences the performance of routing protocols. The source on the left is the only node that generates packets, at a rate of one 1000-byte packet every 2 min. Such packets are then routed to the sink on the right through the relays in between, using either SUN or the flooding protocol.

Fig. 8 shows the throughput in bit/s as a function of the cell side length L for the SUN and the flooding protocols. We note that smaller values of L result in a denser deployment, with nodes that are closer on average. For this reason, the curves show an initially stable behavior: regardless of the variation of the SNR over time, its instantaneous values are likely sufficient to receive the packets without errors. When L increases is no longer the case. Starting from $L = 1600$ m, the higher attenuation makes SNR fluctuations sufficiently strong to corrupt received packets. Both SUN and flooding suffer from this effect, although SUN's capability to recover broken routes maintains the throughput within an acceptable fraction of the maximum achieved when $L \leq 1500$ m. Interestingly, flooding's throughput experiences a local maximum around $L = 2000$ m: this effect is due to a favorable balance between the occurrence of more transmission errors caused by significant SNR variability and interference: as fewer nodes receive a correct version of the packets, fewer replicas are injected in the network, and the reduced interference that results favors the correct delivery of a higher number of packets. For $L \geq 2500$ m, this situation is reverted and SUN achieves a better throughput.

The observations above are corroborated by Fig. 9, showing the end-to-end delivery delay as a function of the cell side length L. This figure proves that SUN's performance suffers when the variations of the SNR are sufficient to disrupt the known routes to the sink. The retransmissions that are triggered as a consequence, as well as the search of new paths, lead to increasingly higher end-to-end delays. On the
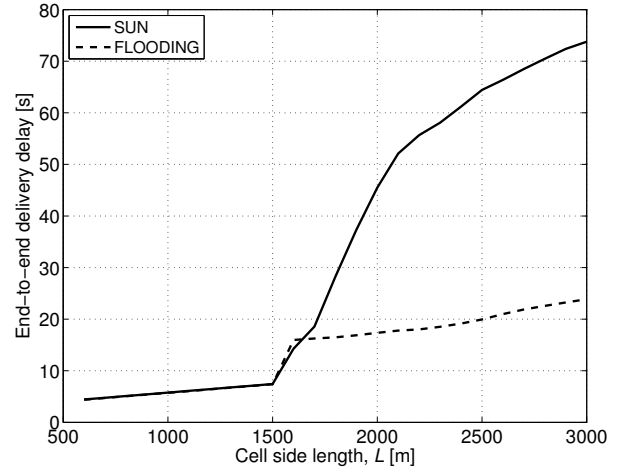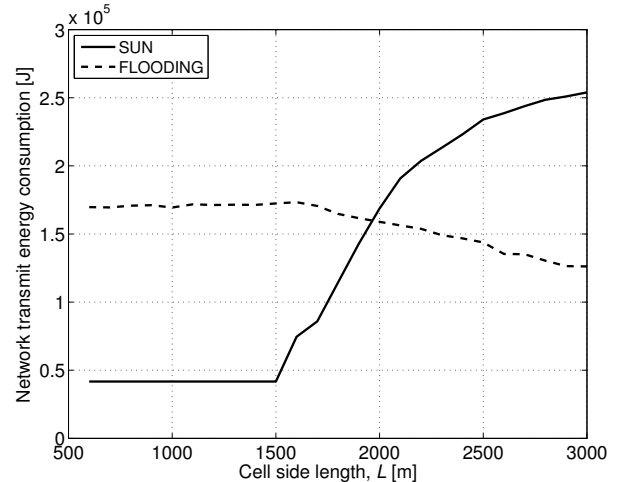
Fig. 10. Transmit energy consumption in the network as a function of the cell side length L for the SUN and the flooding protocols. As discussed for Fig. 9, for $L \geq 1500$ m, the number of route discoveries performed increases: as each discovery resorts to a flooding process, the energy consumed by SUN increases and gradually overcomes the energy consumption of the pure flooding protocol.

contrary, the delay experienced by the flooding protocol is always much lower than SUN's, as flooding simply requires that packets are forwarded, with no control procedure or link-level retransmissions.

As a final study, Fig. 10, which shows the transmit energy consumption in the whole network as a function of L. For this evaluation, we assume that the transmit power consumption is 10 W, akin to that of the WHOI micromodem [21]. Note that we do not consider the energy consumed for reception and idling, as they similarly affect both protocols. Fig. 10 suggests that SUN's path search procedure is effective at reducing the energy consumption, so long as the known path is sufficiently stable. After SNR fluctuations become sufficient

to disrupt routes ($L \geq 1500$ m), SUN must perform route recovery or re-discovery procedures more often, and spends increasingly more energy doing that as L increases. Eventually, SUN's energy consumption overcomes the energy required by flooding, which expectedly decreases: in fact, as L increases the chance of transmissions errors also increases, and leads to the generation of fewer replicas of the same data packets.

To summarize the results, we can conclude that SUN is a good solution for underwater networks as far as the rate of variability in the channel does not result in routes being disrupted faster than the protocol can repair them. However, if the paths are sufficiently stable, the SUN protocol offers very low energy consumption compared to more transmission-intensive approaches such as flooding. The analysis presented in Section III-B helps estimate the average hop distance for which such effect occurs, and is corroborated by the simulation results in this section.

IV. Conclusions

In this paper, we considered routing in underwater networks using source routing and flooding. We showed that the capability of source routing to correctly find routes and use them to deliver packets critically depends on the variability of the channel and node distance. After discussing the channel variability patterns experienced in real experiments, we discussed a method to reproduce the channel variations perceived by non-coherent receivers using the ray tracing. We employed the resulting data set to estimate the hop distance for which source routing reacts too slowly with respect to the rate of variation of the channel. We finally compared the analysis to simulation results, which confirmed this intuition. Our results help understand whether source routing is more convenient than flooding as a function of the size of the network deployment.

References

[1] J. C. Preisig, "Performance analysis of adaptive equalization for coherent acoustic communications in the time-varying ocean environment," *J. Acoust. Soc. Am.*, vol. 118, no. 1, pp. 263–278, 2005.

[2] M. Siderius, M. B. Porter, P. Hursky, V. McDonald, and K. Group, "Effects of ocean thermocline variability on noncoherent underwater acoustic communications," *J. Acoust. Soc. Am.*, vol. 121, no. 4, pp. 1895–1908, 2007.

[3] A. Song, M. Badiey, H. C. Song, W. S. Hodgkiss, M. B. Porter, and the KauaiEx Group, "Impact of ocean variability on coherent underwater acoustic communications during the Kauai experiment (KauaiEx)," *J. Acoust. Soc. Am.*, vol. 123, no. 2, pp. 856–865, 2008.

[4] A. Song, M. Badiey, D. Rouseff, H. C. Song, and W. Hodgkiss, "Range and depth dependency of coherent underwater acoustic communications in KauaiEx," in *IEEE OCEANS 2007 - Europe*, Jun. 2007, pp. 1 –6.

[5] M. Badiey, Y. Mu, J. Simmen, and S. Forsythe, "Signal variability in shallow-water sound channels," *IEEE J. Ocean. Eng.*, vol. 25, no. 4, pp. 492 –500, Oct. 2000.

[6] N. M. Carbone and W. S. Hodgkiss, "Effects of tidally driven temperature fluctuations on shallow-water acoustic communications at 18 kHz," *IEEE J. Ocean. Eng.*, vol. 25, no. 1, pp. 84–94, Jan. 2000.

[7] A. Song, M. Badiey, H. C. Song, and W. S. Hodgkiss, "Impact of source depth on coherent underwater acoustic communications," *J. Acoust. Soc. Am.*, vol. 128, no. 2, pp. 555–558, 2010.

[8] S. Azad, P. Casari, C. Petrioli, R. Petroccia, and M. Zorzi, "On the impact of the environment on MAC and routing in shallow water scenarios," in *Proc. of IEEE OCEANS*, Santander, Spain, Jun. 2011.

[9] F. Guerra, P. Casari, and M. Zorzi, "World Ocean Simulation System (WOSS): a simulation tool for underwater networks with realistic propagation modeling," in *Proc. of WUWNet 2009*, Berkeley, CA, Nov. 2009.

[10] C. Petrioli, R. Petroccia, and J. Potter, "Performance evaluation of underwater MAC protocols: From simulation to at-sea testing," in *Proc. of IEEE OCEANS*, Santander, Spain, Jun. 2011.

[11] B. Tomasi, J. Preisig, G. B. Deane, and M. Zorzi, "A study on the wide-sense stationarity of the underwater acoustic channel for non-coherent communication systems," in *Proc. of European Wireless*, Apr. 2011.

[12] B. Tomasi, G. Zappa, K. McCoy, P. Casari, and M. Zorzi, "Experimental study of the space-time properties of acoustic channels for underwater communications," in *Proc. IEEE/OES Oceans*, Sydney, Australia, May 2010.

[13] W. S. Hodgkiss and J. C. Preisig, "Kauai Acomms MURI 2011 (kam11) experiment," in *Proc. of European Conference on Underwater Acoustics (ECUA)*, Aberdeen, United Kingdom, Jul. 2012.

[14] B. Tomasi, P. J. C., and M. Zorzi, "On the spatial correlation of the channel quality in shallow water," in *Proc. of IEEE OCEANS*, Yeosu, Republic of Korea, May 2012.

[15] B. Tomasi, J. Preisig, and M. Zorzi, "On the predictability of underwater acoustic communications performance: the KAM11 data set as a case study," in *Proc. of ACM WUWNet*, 2011.

[16] M. Porter *et al.*, "Bellhop code." [Online]. Available: http://oalib.hlsresearch.com/Rays/index.html

[17] F. Jensen, W. Kuperman, M. Porter, and H. Schmidt, *Computational Ocean Acoustics*, 2nd ed. New York: Springer-Verlag, 1984, 2nd printing 2000.

[18] N. Baldo, M. Miozzo, F. Guerra, M. Rossi, and M. Zorzi, "Miracle: The multi-interface cross-layer extension of ns2," *EURASIP Journal on Wireless Communications and Networking*, vol. 2010, no. 1, pp. 761–792, 2010.

[19] R. Urick, *Principles of Underwater Sound*. New York: McGraw-Hill, 1983.

[20] M. Stojanovic, "On the relationship between capacity and distance in an underwater acoustic communication channel," *ACM Mobile Comput. and Commun. Review*, vol. 11, no. 4, pp. 34–43, Oct. 2007.

[21] L. Freitag, M. Grund, S. Singh, J. Partan, P. Koski, and K. Ball, "The WHOI micro-modem: An acoustic communications and navigation system for multiple platforms," in *Proc. of MTS/IEEE OCEANS*, Washington, DC, Sep. 2005.